Comprehensive study on compositional modification of Tb3+ doped zinc phosphate glass

by Sulhadi 50

Submission date: 02-Aug-2022 09:44AM (UTC+0700)
Submission ID: 1877935653
File name: 2018_Solid_State_Yacoob_dkk.pdf (1,017.34K)
Word count: 6660
Character count: 32555

Accepted Manuscript

Comprehensive study on compositional modification of Tb^{3+} doped zinc phosphate glass

S.N.S. Yaacob, M.R. Sahar, E.S. Sazali, Zahra Ashur Mahraz, K. Sulhadi

PII: S1293-2558(18)30001-3

DOI: 10.1016/j.solidstatesciences.2018.05.006

Reference: SSSCIE 5692

To appear in: *Solid State Sciences*

Received Date: 18 January 2018

Revised Date: 15 May 2018

Accepted Date: 15 May 2018

Please cite this article as: S.N.S. Yaacob, M.R. Sahar, E.S. Sazali, Z.A. Mahraz, K. Sulhadi, Comprehensive study on compositional modification of Tb^{3+} doped zinc phosphate glass, *Solid State Sciences* (2018), doi: 10.1016/j.solidstatesciences.2018.05.006.

Graphical Abstract

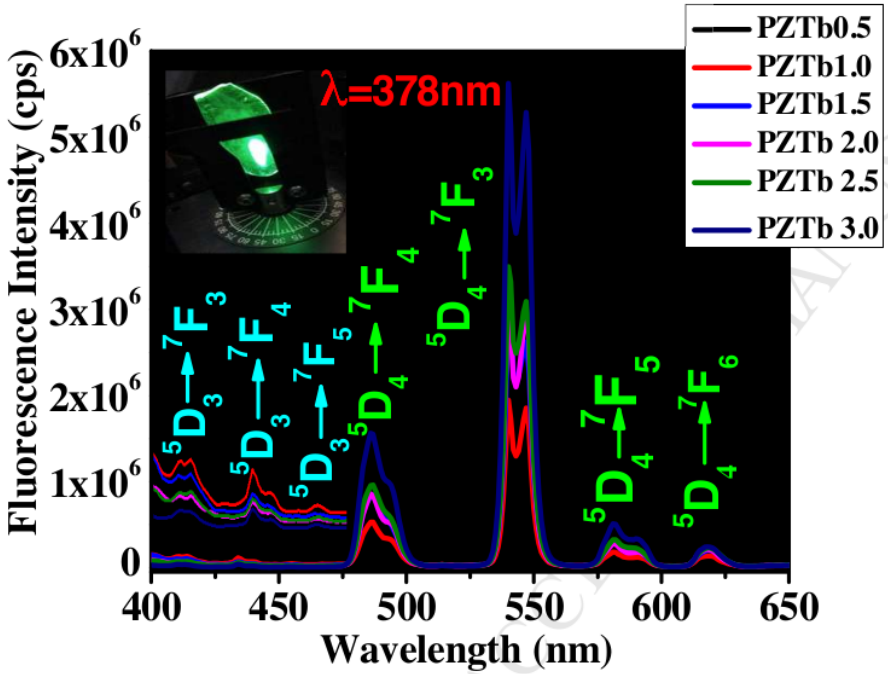

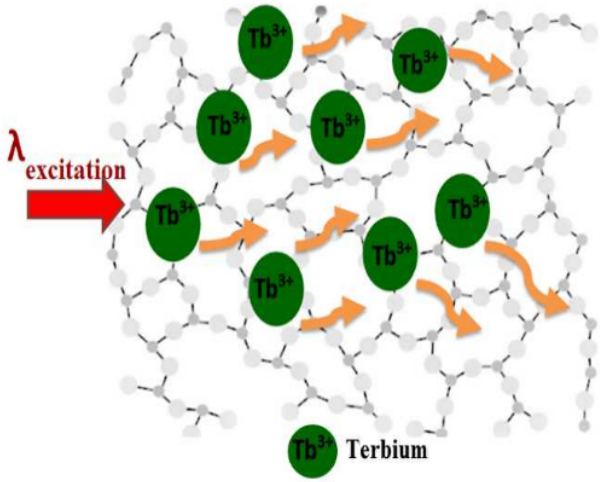

Comprehensive study on compositional modification of Tb^{3+} doped zinc phosphate glass

S.N.S. Yaacob[1] & M.R. Sahar[1] & E.S. Sazali[1] Zahra Ashur Mahraz[1] & K. Sulhadi[2]

[1] *Advanced Optical Materials Research Group, Department of Physics, Faculty of Science, Universiti Teknologi Malaysia, 81310 Skudai, Johor, Malaysia*

[2] *Department of Physics, Faculty of Mathematics and Natural Science, Universitas Negeri Semarang, Jl. Raya Sekaran, Gunungpati Semarang 50229 Indonesia*

Abstract: Series of glass composition (60-*x*) P_2O_5 -30 ZnO –(*x*) Tb_2O_3 where x= 0.5, 1.0, 1.5, 2.0, 2.5 and 3.0 mol % are prepared by conventional melt quenching technique. X-Ray Diffraction (XRD), FTIR, UV-Vis-NIR and the photoluminescence (PL) spectroscopy are used to characterize the physical, structural and optical behavior of the glass sample. The XRD pattern confirms the amorphous nature and DTA verified the thermal stability of all the glass samples. Glass with 1.5 mol % of Tb_2O_3 possesses the highest thermal stability. Glass density is found to increase proportionally with increasing amount of Tb^{3+} while the molar volume behaves reversely. Six main IR absorption bands centered at about 540, 748, 891, 1085 and 1294 cm^{-1} are evidenced. The UV-Vis NIR absorption spectra reveals the absorption center band at about 540, 376, 488 and 1920 nm corresponding to the absorption from $^7F_6$ ground state to various excited state of Tb^{3+} ion. The optical band gaps for direct and indirect transition are in the range 4.53 -5.07 eV and 4.30 eV-4.56 eV respectively. The Urbach energy decreases with the increasing concentration of Tb_2O_3. The PL emission spectra reveals several prominent peaks at 413, 435, 457, 488, 540, 585 and 620 nm due to electronic transition from $^5D_3 \rightarrow {}^7F_5$, $^5D_3 \rightarrow {}^7F_4$, $^5D_3 \rightarrow {}^7F_3$, $^5D_4 \rightarrow {}^7F_6$, $^5D_4 \rightarrow {}^7F_5$, $^5D_4 \rightarrow {}^7F_3$ and $^5D_4 \rightarrow {}^7F_5$ respectively.

Keywords: **Terbium oxide, phosphate glass, optical properties, physical properties**

1.0 Introduction

Recently research on glass has potential to develop a new interest in material engineering. Choosing appropriate glass host is favorable key role in the luminescence properties along with physical and optical of active ions [1,2]. Phosphate as a glass host creates many advantages owing to its unique properties [3,4]. For instance high thermal expansion for sealing glass purpose, melt at low temperature, possess high ultraviolet (UV) and far infrared transmissions for optical data transmission application [5–7]. Besides that, phosphate glasses are excellent materials to accommodate with other modifier such as oxide materials and rare earth ions [8,9]. The of the network modifier Zn^{2+} altered the phosphate glass structure by forming non-bridging oxygen (NBOs) and improved the chemical durability of phosphate glass [10].

The photoluminescence characteristics of rare earths doped into various kind of hosts have been extensively studied in the past due to its wide range of its application such as optical data storage and medical treatment [11] .This glasses recognized as fascinating materials due to the f–f transition lies on the visible and near-infrared (NIR) region [12]. The unique properties of lanthanide ions assigned them as luminescent indicator group for laser development [13]. Among all lanthanide ion, progressive research has been focus on producing green laser by Er^{3+} doped glass pumped with 0.8 μm laser diodes [14]. However, the up-conversion process results in energy lost via non radiative relaxation process and consequently decrease the efficiency of the system [15]. Trivalent rare earth ions such as terbium ion, Tb^{3+} display efficient green emission, when doped with phosphor material [16]. The efficient of green laser of the Tb^{3+} are due to transition from $^5D_4$ and $^5D_3$ excited states with large gap between the energy level assists the radiative transition substantially easily produced laser output [17]. In sequence, optimum concentration are important to emphasized in order to avoid from quenching and enhanced stability [18]. Furthermore the luminescence enhancement and quenching are crucial to discussed in briefly.

Hence, this paper reports the effects of Tb_2O_3 composition variation on the physical, structural and optical properties of binary zinc phosphate glasses. Seven samples of zinc phosphate glass doped terbium were prepared with variation concentration of Tb_2O_3 range from 0.0 mol % to 3.0 mol %. The functional groups present in the glass system are well explored. The thermal properties are paramount to indicate the glass stability. Besides that, the energy band gap and Urbach energy refractive index and polarizability are used to describe the optical behavior of the glass. Finally, the radiative properties responsible for

enhancement of Tb^{3+} are briefly discussed.

2.0 Experimental

2.1 Glass preparation

Series of glass composition (60-x) P_2O_5 -30 ZnO –(x) Tb_2O_3 where x = 0.0, 0.5, 1.0 1.5, 2.0, 2.5 and 3.0 mol % are prepared using conventional melt quenching method. 15 g of glass constituents contain analytical grade powder of P_2O_5 (Sigma Aldrich 99.99%), ZnO (Sigma Aldrich 99.99%), Tb_2O_3 (Sigma Aldrich 99.99%) are mixed together in the alumina crucible and melted in a furnace at 1100°C for 1 hour 30 minutes. Once the required viscosity is achieved, the melt is poured into a steel plate and annealed at 300°C for 4 hours to assure the release of stress. The transparent glass sample is cooled down to room temperature and polished to a surface with 1 mm x 1 mm dimension using a diamond paste. The nominal compositions of samples are listed in Table 1.

Table 1: Nominal compositions of P_2O_5 – ZnO – Tb_2O_3 glass

Sample	Glass compositions (mol %)			Remarks
	P_2O_5	ZnO	Tb_2O_3	
PZTb 0	60.0	40	0.0	Transparent
PZTb 0.5	59.5	40	0.5	Transparent
PZTb 1.0	59.0	40	1.0	Transparent
PZTb 1.5	58.5	40	1.5	Transparent
PZTb 2.0	58.0	40	2.0	Transparent
PZTb 2.5	57.5	40	2.5	Transparent
PZTb 3.0	57.0	40	3.0	Transparent

2.2 Glass characterization

The XRD spectra are recorded using X-Ray diffractometer (Model: PAN analytical X'PertPro) with CuK_α monochromatic radiation source (λ=1.54187 Å) at 40 kV and 30 Ma in 2θ range of 10°C Scanning). The UV –Vis NIR absorption measurement in the range 200 nm – 2000 nm are carried out using Shimadzu spectrophotometer (Model: UV -3101 PC Scanning). The energy band gap and Urbach energy values are determined by UV-VIS spectrophotometer. The emission spectra in the excitation range of 400- 650 nm are determined using Perkin Elmer LS-5S photoluminescence (PL) spectrophotometer. For IR measurement, the glasses powdered are mixed with KBr and press under high pressure to obtain thin pellet. The IR spectra are obtained by Perkin Elmer Spectrum.

The glass density determined by using Archimedes Principle as stated in equation

$$\rho = \frac{W_a}{W_a - W_L}(\rho_x) \quad (1)$$

where ρ_x is the density of immersion liquid. W_a is the weight of the glass in air and W_L is the weight of the sample when immersed in immersion liquid. The molar volumes V_m is calculated by using the obtained density and weight of one mole of sample by using equation

$$V_m = \sum i \frac{x_i M_i}{\rho} \quad (2)$$

where x_i and M_i refers to the molar fraction and molecular weight of the component *i*th respectively.

The ionic packing density V_t in (m^3/ mol %) calculated by the equations

$$V_t = \left(\frac{1}{V_m}\right) \sum (V_m \; x_m) \quad (3)$$

where V_m is the molar volume and x_i is the molar fraction (in mol %) as in equations

$$V_i = \frac{4\pi N_A}{3} [X r_m^{\,3} + Y r_o^{\,3}] \quad (4)$$

where N_A is the Avogadro's number (in mol^{-1}) r_m and r_o are the shanon's ionic radius of metal and oxygen

Mott and Davis proposed that the absorption coefficient α(ν) as a function of photon energy can be written as equation

$$\alpha(\nu) = \frac{B(h\nu - E_{opt})^m}{h\nu} \quad (5)$$

where *B* is a constant E_{opt} is the optical energy band gap. For direct transition m=1/2 or 3/2 and for indirect transition, m=2 or depends on whether the transition is forbidden or allowed [19] . The optical absorption edge of amorphous determined by the band tail where

the exponential curve of absorption coefficient versus photon energy was described by the Urbach as equation

$$\alpha(h\nu)=B\ exp(\frac{h\nu}{\Delta E}) \quad (6)$$

where B is constant and ΔE is the Urbach energy which indicated the width of the band tail of localized states in the band gap.

The refractive index can be calculated by the equation

$$\frac{n^2+1}{n^2-1}=1-\sqrt{\frac{E_{opt}}{20}} \quad (7)$$

The Lorentz Lorents equation are used to calculate the molar refractivity R_m and electronic polarizability α_m as follows

$$R_m=\frac{n^2-1}{n^2+1}\ (V_m) \quad (8)$$

$$\alpha_m=(\frac{3}{4\pi N_a})\ R_m \quad (9)$$

3.0 Result & Discussion

This section will focus on the results that have been obtained throughout the experimental work followed by some discussions related to the results.

3.1 XRD analysis

The typical X-ray diffraction of terbium doped zinc phosphate glass shown in Fig. 1 The presence of broad hump at 20 °to 30°indicates the amorphous nature of the prepared glass

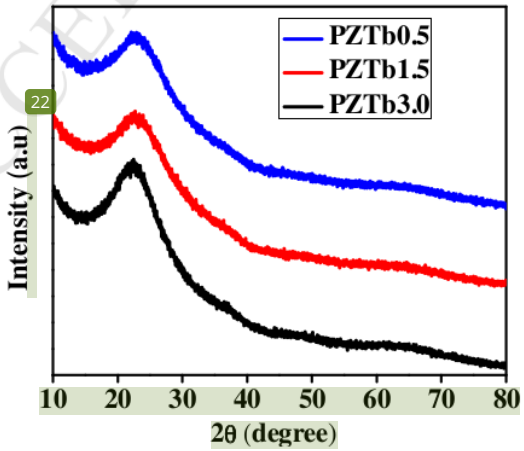

Figure 1: XRD pattern for glass sample containing Tb_2O_3

3.2 EDX analysis

Figure 2 illustrate EDX spectrum for glass sample PZTb 3.0.The several sharp peaks reveal the presence of elements such as P, Zn, O and Tb. The analysis on the composition has been done and the results are tabulated in **Table 2.** The differences between the nominal and actual percentage of elements is owing to EDX analysis which quantifies elements by calculating the area under the peak of each identified element. The EDX analysis depends on the accelerating voltage of the beam to produce the spectrum and performs calculations to create sensitivity factors that will transform the area under the peak into weight or atomic percent. The probability of an X-ray escaping the sample for detection and measurement is governed by the energy of the X-ray and density of material it has to pass through. Nevertheless, the X-rays which are generated by any atom in the sample are emitted in any direction where some of them may be absorbed by the sample. Thus this effects will reduced the accuracy of the elemental traces in inhomogeneous and rough samples [20].

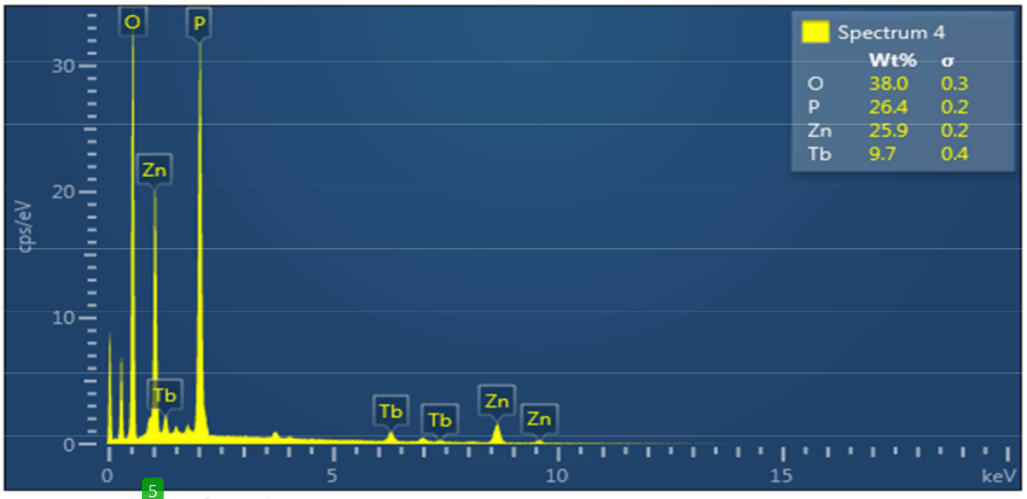

Figure 2: EDX spectrum of glass sample PZTb 3.0

Table 2: The actual and nominal composition glass sample

Sample		P_2O_5	ZnO	Tb_2O_3
PZTb0.0	Nominal (mol%)	60.0	40.0	-
	Actual (mol%)	70.13	29.77	-
PZTb0.5	Nominal (mol%)	59.5	40.0	0.5
	Actual (mol%)	69.44	29.64	0.92
PZTb1.0	Nominal (mol%)	59	40	1.0
	Actual (mol%)	69.00	29.50	1.61
PZTb1.5	Nominal (mol%)	58.5	40	1.5
	Actual (mol%)	68.20	30.08	1.72
PZTb2.0	Nominal (mol%)	58.0	40.0	2.0
	Actual (mol%)	66.65	30.44	2.91
PZTb2.5	Nominal (mol%)	57.5	40.0	2.5
	Actual (mol%)	66.55	30.35	3.10
PZTb3.0	Nominal (mol%)	57.0	40.0	3.0
	Actual (mol%)	65.04	30.28	4.67

3.1.4 IR Spectra

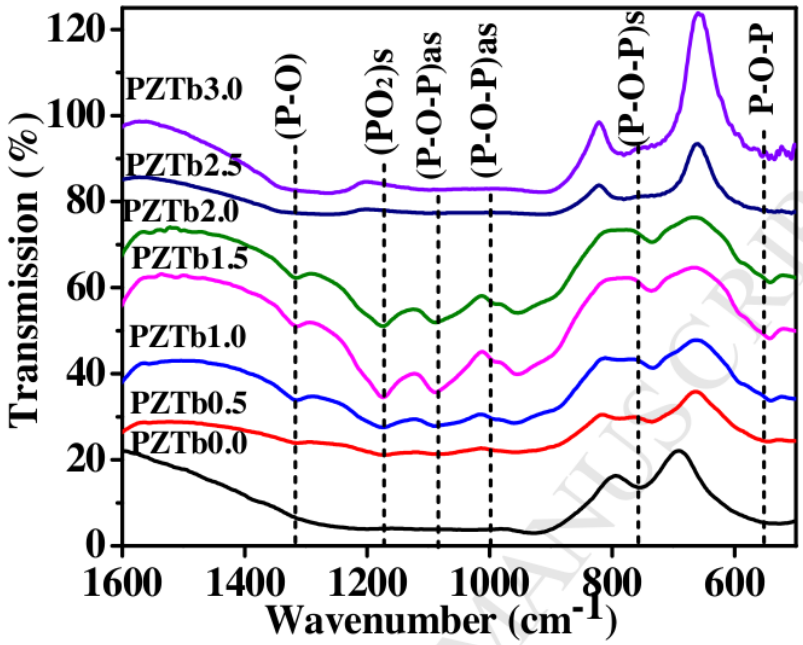

Figure 3: IR Spectra of zinc phosphate glass at various concentration of Tb_2O_3

The FTIR spectra of the proposed glass are shown in the **Figure 3** and their corresponding IR bands and the assignments of vibrational bands are tabulated in **Table 3.** The present results displays are in the same manner with previous studies. Six significance bands are observed. Hence the IR absorption spectra are as follows .The characteristic IR bands center at 550 cm^{-1} ascribed to the distortion of P-O-P glass network [4]. The peaks observed in the of range 720cm^{-1} to 748$cm^{-1}$are associated with the stretching vibration of bridging oxygen [17,21].The bands at around 790–815 cm^{-1} are due to symmetric stretching vibrations of P–O–P rings [22] .The bands lie around at 1000 cm^{-1} to 1012cm^{-1} are attributed to the asymmetric stretching vibration in P-O-P linkages.The absorption bands lie within this range 1119cm^{-1} to 1126cm^{-1} is due to the asymmetric stretching vibration in P-O in Q_2 units. The band appeared at 1170 cm^{-1} is assigned to the PO_2 symmetric stretching mode, $(PO_2)s$ [23]. The observed increment in the intensity of IR band around 1264–1345cm^{-1} is assigned to the symmetric stretching vibration in P-O bond attributed to the addition of Tb_2O_3 bond. It is observed that Q_2 species vibration give rise to sufficiently intense IR features compares to the

vitreous network of P_2O_5 which mainly made up of Q_3. This indicates that incorporation of zinc oxide to phosphate network causes the replacement of Q_3 to Q_2 sites [24].

Table 3: IR bands and their assignments for all studied glass samples

Characteristic band (cm^{-1})	Band assignment
550	Distortion of P-O-bond
720-748	Stretching vibration of bridging oxygen
790–815	Symmetric stretching vibrations of P–O–P rings
1000-1012	Asymmetric stretching vibration in P-O-P linkages.
1119-1026	Asymmetric stretching vibration in P-O-P bond
1169-1174	Symmetric stretching mode PO_2
1264-1345	Asymmetric stretching vibration in P-O bond

3.2 DTA analysis

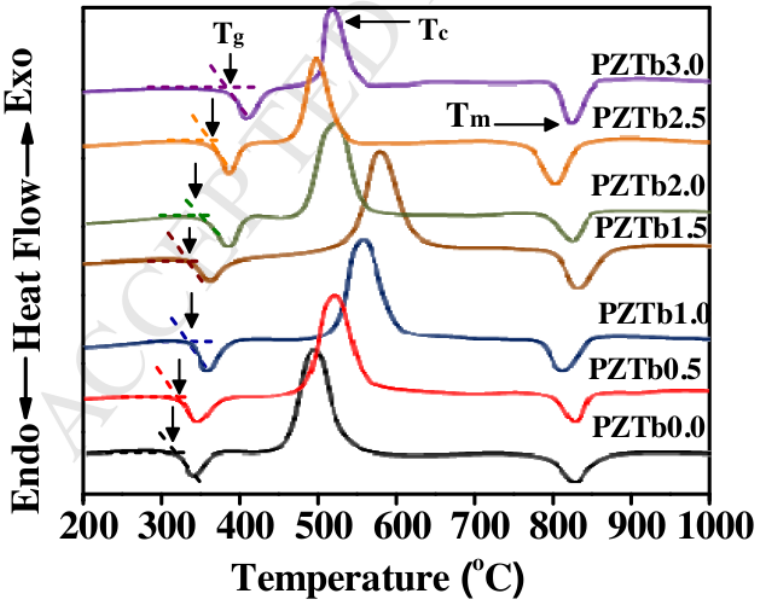

Figure 4 Typical DTA curve of zinc phosphate glass at various concentration of Tb_2O_3

Figure 4 illustrates the typical DTA curve in the range 200°C to 1000°C of zinc phosphate glass doped with varying content of Tb^{3+} .The values of T_c (crystallization temperature) T_g (glass transition) and T_m (melting temperature) are tabulated in **Table 4**. The T_g and T_c values are observed to increase with the increase in Tb_2O_3 up to 3.0 mol %. The results presented are in good agreement with the previous study done by Dousti *et al*. [25]. Increase in the T_g governed by the properties of anisotropies of Q^1 and Q^2 sites [26] .The thermal stability calculated by the difference $T_s = T_c - T_g$ reflect the glass formation ability .Previous literature stated that the glass considered stable when the T_s is greater than 100°C [27]. The stability of the glass T_s increases with increase of Tb^{3+} up to 1.5 mol% from 175 to 235 °C reflect improvement against crystallization [28]. Notably, this is due to the higher volume of Tb^{3+} prone to dominate in the glass structure compare to P_2O_5 [29]. However beyond 1.5 mol% of Tb^{3+}, the glass stability decreases. The unusual behavior trends describe by Ahmina *et al*. as discrete alterations in the glass network as the glass unit tends to restructure when beyond T_g [30].

Table 4: Thermal properties of zinc phosphate glass doped with Tb^{3+}

Glass code	Tc (°C)	Tg (°C)	Tm (°C)	Ts (°C)
PZTb 0.5	324	499	809	175
PZTb 1.0	334	558	814	224
PZTb 1.5	344	579	812	235
PZTb 2.0	357	524	818	167
PZTb 2.5	365	501	808	136
PZTb 3.0	380	514	816	134

3.3 Density, molar volume and ionic packing density

The introduction of Tb^{3+} into the glass network increases the glass density from 2.86 gcm^{-3} to 3.24 $gcm^{-3}$and reduce the molar volume from 40.08 cm^3 mol^{-1} to 37.71 cm^3 mol^{-1} as depicted in **Figure 5** and tabulated in **Table 5**. The larger molar mass of Tb_2O_3 (365.85 $gmol^{-1}$) compared to the molar mass of P_2O_5 (94.97 $gmol^{-1}$) are responsible for this increment [25]. The addition of more Tb^{3+} ions develops the non-bridging oxygen and change the glass structure. Thus, the molecules become more compact and denser as the Tb^{3+} ion occupied the interstitial within the glass network. The molar volumes tends to reduce with the increase of Tb^{3+}.The reduction of molar volume due to the replacement of larger Tb^{3+} (0.92 Å) ion with

smaller P^{5+} ion (0.31 Å) thus alter the network bonding [26]. The ionic packing density is increasing with increasing concentration of Tb_2O_3 up to 0.671.The increment of ionic packing density mainly due to the inclusion of higher density of Tb_2O_3 (8.27 gcm^{-3}) at the expense of lower density of P_2O_5 (2.31 gcm^{-3}) [19].

Table 5: Physical properties of zinc phosphate glass doped with varying content of Tb^{3+}

Physical Properties	PZTb0.0	PZTb0.5	PZTb1.0	PZTb1.5	PZTb2.0	PZTb2.5	PZTb3.0
Density ρ (g/cm^3)	2.86	3.01	3.16	3.20	3.24	3.20	3.24
Molar Volume (cm^3mol^{-1})	40.08	39.87	39.85	38.31	38.30	37.83	37.71
Ionic packing density V_t	0.741	0.641	0.643	0.664	0.665	0.670	0.671
Concentration of Tb ion (cm^3) × 10^{18} ions	0.00	0.76	1.58	2.38	3.19	3.87	4.74

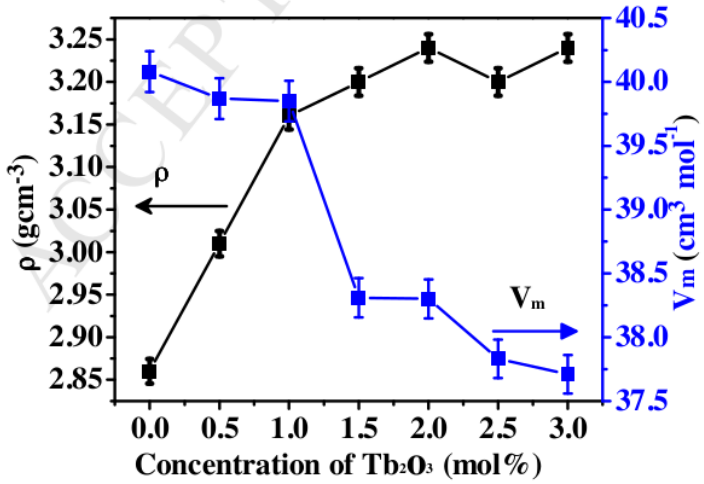

Figure 5: Tb_2O_3 concentration dependent density and molar volume

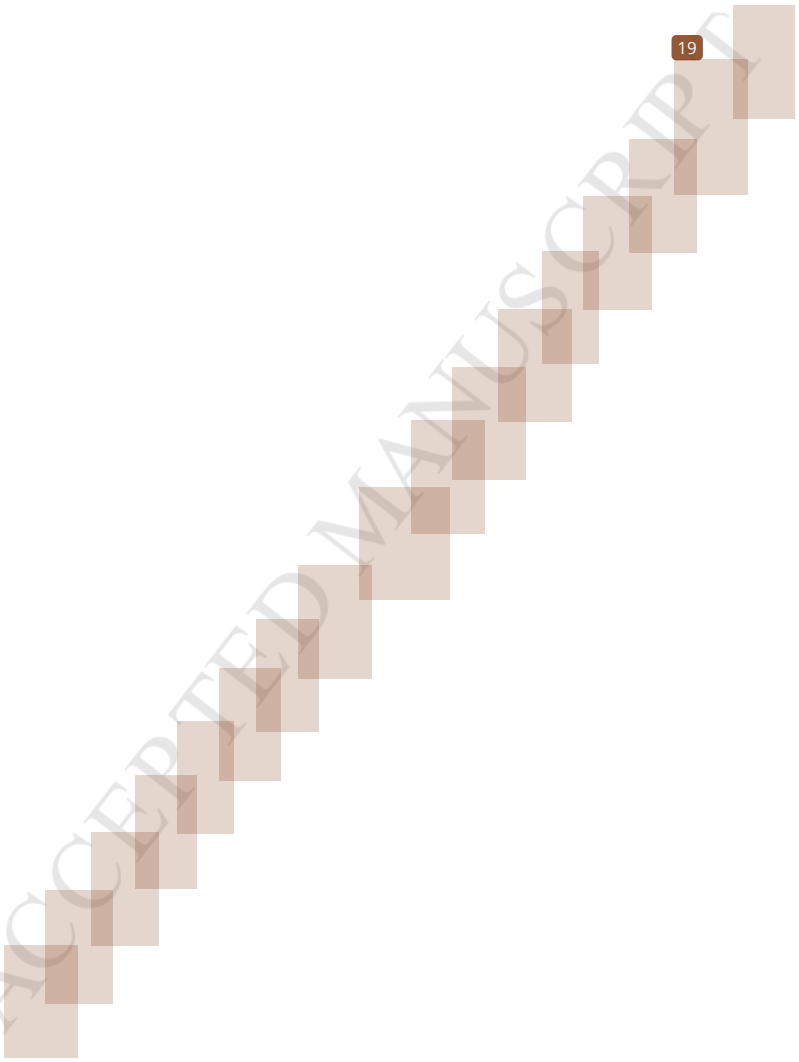

3.4 Absorption properties

The absorption spectra are used to figure out the electronic transition and energy band gap of the amorphous semiconductor [31]. The optical absorption spectra in the range of 200 –2500 nm is shown in **Figure 6**. All bands are lies in the visible and near infrared region. Sharp absorption peak observed at 248 nm is due to 4f-5d transition [32]. Other bands are observed at wavelength 318 nm 350 nm 378 nm 484 nm 1894 nm and 2224 nm are due to the transition from ground state $^7F_6$ to several transition $^7F_6 \rightarrow {}^5D_0$ $^7F_6 \rightarrow {}^5D_1$, $^7F_6 \rightarrow {}^5D_2$, $^7F_6 \rightarrow {}^5D_3$, $^7F_6 \rightarrow {}^5D_4$ and $^7F_6 \rightarrow {}^7F_{0,1,2}$ $^7F_6 \rightarrow {}^7F_3$ respectively [12,25,33]. It is noticeable that the wider peak at 2224 nm are due to the overlapping of several transition from ground state $^7F_6$ to $^7F_0$, $^7F_1$ and $^7F_2$ [17]. Noteworthy that all the transition present in the absorption bands are accordance with the selection rules $\Delta S = 0$, $L \leq 6$ and $\Delta J, \leq 6$ [34]. The absorption band at transition ($^7F_6 \rightarrow {}^5D_4$) displays weakest intensity comparable to other transition showing fair intensity. It is also observed that the absorption intensity increasing monotonically with increasing concentration of Tb_2O_3. Furthermore, the cut off wavelength is shifted to higher wavelength from 269 nm to 286 nm with increasing concentration of Tb_2O_3. The observed shifting to higher wavelength is due to more formation of non-bridging oxygen as more Tb_2O_3 added in the glass system.[35] The distribution of electron in non- bridging oxygen is more polarizable then the bridging oxygen[36].

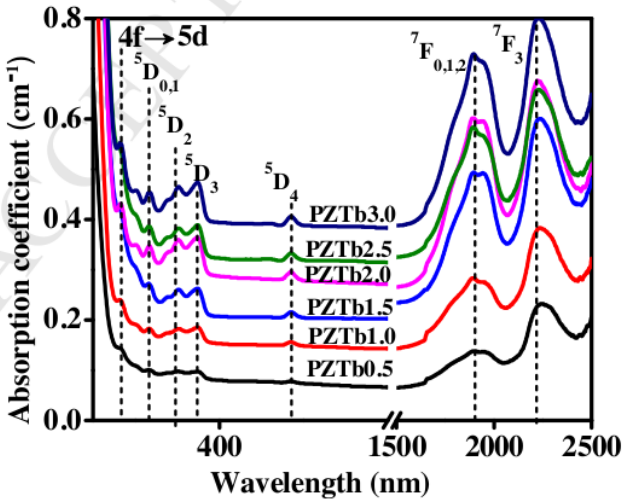

Figure 6: Absorption spectra of zinc phosphate glass at various concentration of Tb_2O_3

3.4 Energy band gap and Urbach energy

Figure 7 shows that the optical energy band gap decreases with increasing concentration of Tb_2O_3. Both the direct and indirect energy band gap tends to decrease from 4.77 eV and 4.57 eV to 4.56 eV and 4.50 eV respectively. The results presents are in the same order as those reported in the previous literature for aluminum silicate doped terbium glasses [37]. They found out that the energy band gap lies in the range 4.78 -4.41 eV. The decrease in energy band gap is attributed to the decrease in average bond energy. This is as more Tb^{3+} is added up to 3.0 mol % the compactness of the glass network decrease due to the formation of non-bridging oxygen (NBO). However, as we compare the energy band gap of glass PZTb0 and PZTb0.5 the energy band gap seems to increase from 3.44 eV to 4.59 eV. The increase in energy band gap correlates with the facts of reduction of non-bridging oxygen due to the introduction of Tb_2O_3 into the glass system.

Besides that, the value of Urbach energy decreases with introducing Tb^{3+} ion into the glass network. Adding more Tb^{3+} ion into the matrix of glass host will create more number of non-bridging oxygen (NBOs) [26]. On the other hand, the decrease in the value of Urbach energy indicates that the degree of disorderness decrease with increasing concentration of Tb^{3+} as reported from the previous workers [7,36,38]

3.5 Refractive index and polarizability

The refractive index with different concentration of Tb_2O_3 is tabulated in **Table 6** and depicted in **Figure 7**. At lower concentration of Tb_2O_3 from ie: 0.5 % up to 1.0 mol%, the refractive index is kept constant at 2.07. However, when the concentration of Tb_2O_3 is increase up to 3.0 mol %, the refractive index increases. The increment is due to the highly polarize of non-bridging oxygen in the glass network. Besides that, the gradual increment of refractive index might also due to the structural disordered in the glass network. As the Tb^{3+} ions are introduced at the interstitial site of the glass network the P-O-P bond is shortened then results in the disorderness of the glass network.

From **Table 5**, it can be seen that the electronic polarizability decreases with the increasing concentration of Tb_2O_3. The electronic polarizability decrease as the field strength is increased. A similar results have also been reported elsewhere [39]. However in this case, the electronic polarizability tends to decrease. This could be due to the low concentration of modifier.

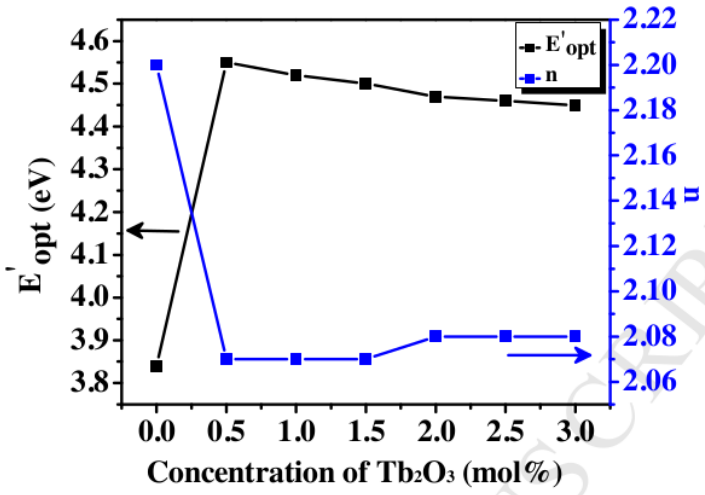

Figure 7:Tb_2O_3 concentration dependent E'_{opt} and n

Table 6: Tb_2O_3 concentration dependent optical properties

Optical Properties	PZTb0	PZTb0.5	PZTb1.0	PZTb1.5	PZTb2.0	PZTb2.5	PZTb3.0
Phonon cut off wavelength λ (nm)	316	269	273	278	282	285	286
Refractive index n	2.20	2.07	2.07	2.07	2.08	2.08	2.08
Molar refractivity , R_m	19.44	24.78	24.76	23.81	23.91	23.62	23.62
Electronic polarizability α $\times 10^{-24}$ (cm^3)	0.77	0.98	0.98	0.94	0.94	0.93	0.93
Direct band gap (eV)	4.50	4.77	4.72	4.68	4.66	4.65	4.64
Indirect band gap (eV)	3.84	4.55	4.52	4.50	4.47	4.46	4.45
Urbach energy (eV)	0.23	0.28	0.26	0.23	0.21	0.19	0.19

3.6 Luminescent properties

Generally, the Tb $^{3+}$ has interesting luminescent performance. Emission spectra of Tb^{3+} doped zinc phosphate glasses in various composition of Tb^{3+} (0.5, 1.0, 1.5, 2.0, 2.5 and 3.0 mol%) shown in **Figure 8**. The emission peak signify two color region which are blue lies in the wavelength 400-460 nm and strong green emission lies in the wavelength 460 nm -650 nm. All these peaks do not shows any shifting peak since the ZnO does not play any role in radiative relaxation as discuss by Hsu and co-workers [40]. From all these bands the band $^5D_4 \rightarrow {}^7F_5$ which in green spectral region transition remarks the highest intensity compared to the other peaks as observed in **Figure 9(a)** and these results are in same manner reported in the previous literature [41]. The emission from ^{5} D_4 to ^7F_j increases with the increment of Tb^{3+}. Meanwhile from **Figure 9(b),** it can be seen that the fluorescent intensity for band $^5D_3$ transition are present and gradually increases from 0.5 mol % to 1.0 mol% of Tb^{3+} but decrease significantly up to 3.0 mol% .Notably from the previous study done by N.S Husain *et al*., incorporation of Tb^{3+} in silicate glass, ion in pair causes absence of blue emission [42]. This signify that our PZTb glass possible producing strong green emission compare to terbium doped silicate glass since our glass has well distribution of Tb^{3+} [43]

The significance observed in quenching of emission $^5D_3$ and enhancement of $^5D_4$ can be discussed elaborately through the interaction of light with Tb^{3+}. **Figure 10** depicts the schematic energy level diagram of Tb^{3+} in zinc phosphate glass. Upon the excitation of Tb^{3+} at wavelength 378 nm, the electron are excited from the ground state $^7F_0$ to the higher energy state $^5D_3$ then relaxed radiative and non radiatively. The radiative decay from $^5D_3$ to lower level $^7F_5$, $^7F_4$ and $^7F_3$ produce several emission bands at 413 nm, 435 nm and 458 nm. Furthermore, the cross relaxation process described by

$$^5D_3 + {}^7F_6 \rightarrow {}^5D_4 + {}^7F_0$$

radiates the $^5D_4$ state and produce several emissions at 488 nm, 548 nm, 588 nm and 620 nm to $^7F_6$, $^7F_5$, $^7F_4$ and $^7F_3$.The cross relaxation phenomenon is due to the resonant energy transfer since the energy difference between $^5D_3$ and $^5D_4$ are same with the energy level between $^7F_6$ and $^7F_0$.The cross relaxation process are more prominent at higher concentration of Tb^{3+} ion due to reduction of interionic distance [44].

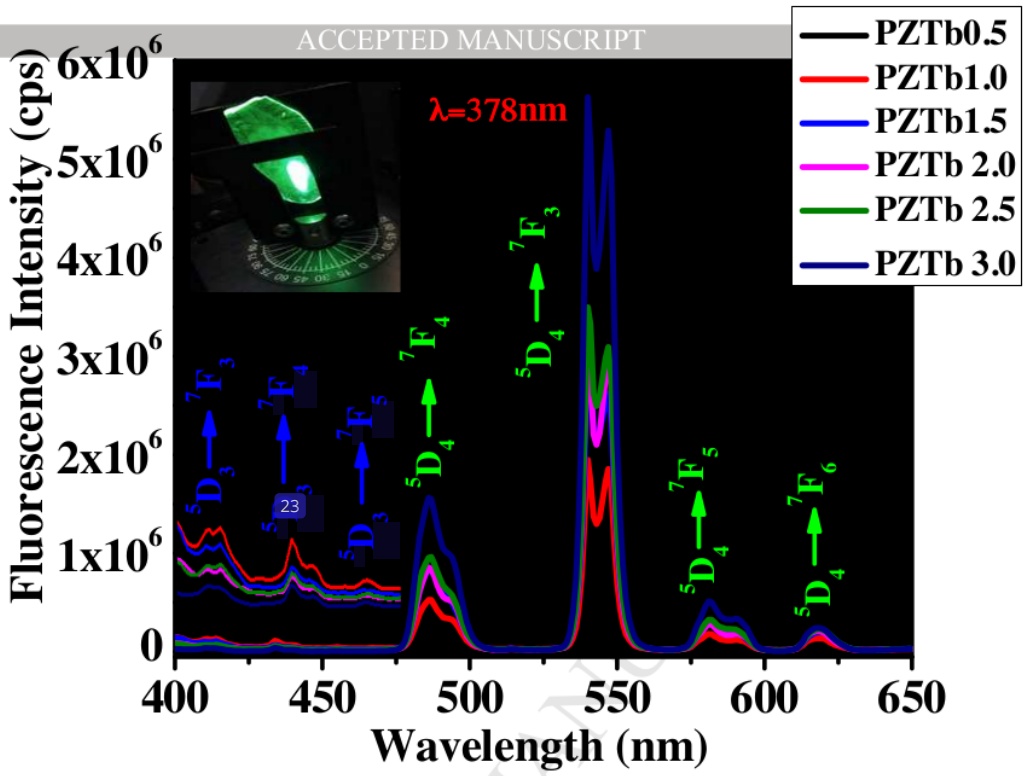

Figure 8: The emission spectra of zinc phosphate glass containing various composition of Tb_2O_3

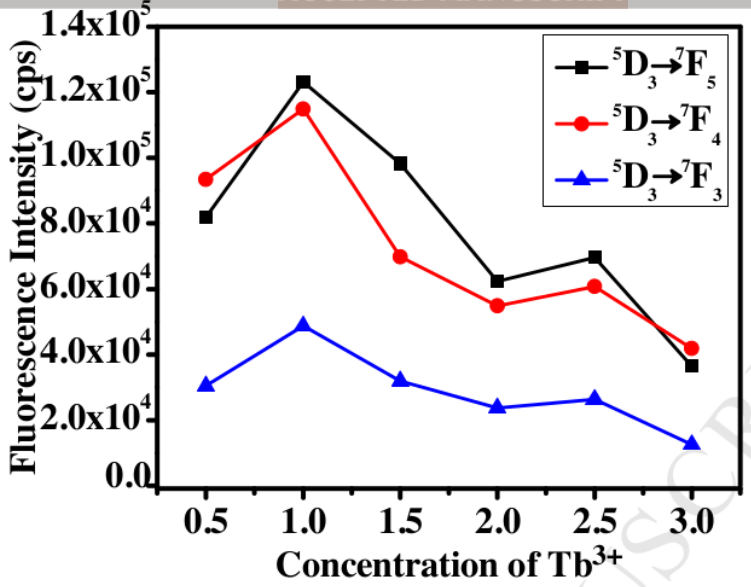

(a)

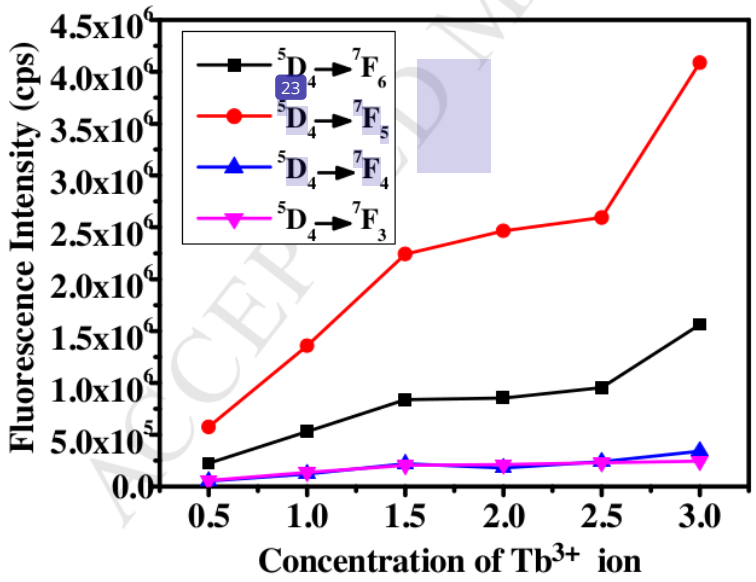

(b)

Figure 9: The intensity of (a) $^5D_3$ and (b) $^5D_4$ transition with variation of Tb^{3+} concentration

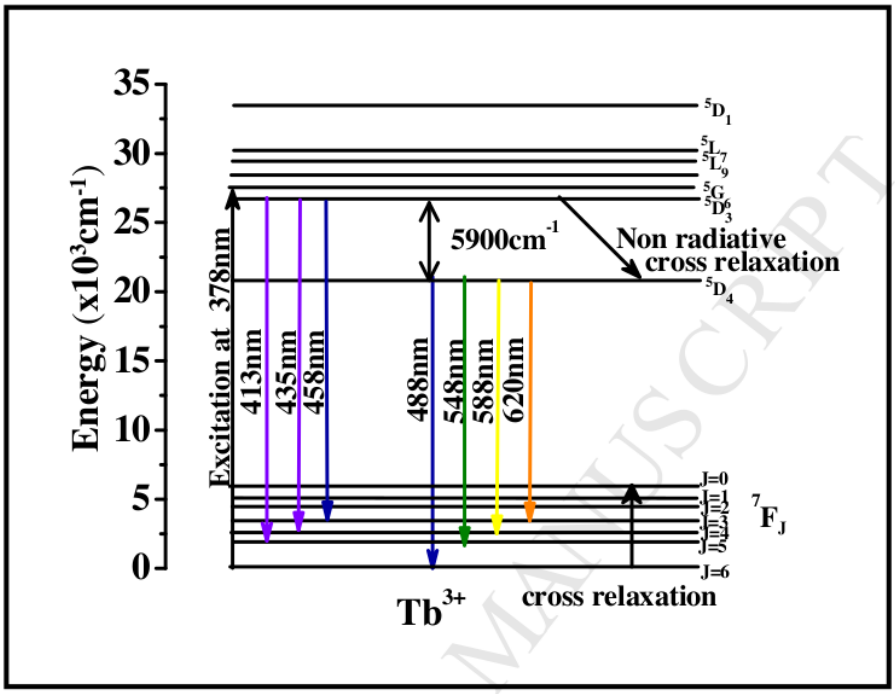

Figure 10: Schematic energy level diagram of Tb^{3+} in zinc phosphate glass.

Conclusion

Zinc phosphate glasses with various Tb^{3+} concentration (0-3.0 mol %) are successfully prepared using melt quenching technique. The terbium concentration- dependents physicals, structural, optical and luminescent properties are determined. The introduction of Tb^{3+} in the glass increases the glass transition temperature. Glass with 1.5 mol % of Tb^{3+} possesses the highest stability. The increase in the density of zinc phosphate glass is due to the substitution of Tb_2O_3 (high molar mass) by P_2O_5 (lower molar mass). The direct and indirect energy band gap decrease with increasing concentration of Tb^{3+}. The decrease in Urbach energy with Tb^{3+} content is due to disorderness in the glass structure. The quenching of fluorescence intensity of $^5D_3$ states at concentration of more than 1.0 mol % of Tb^{3+} is due to the cross relaxation mechanism. The fluorescence intensity of $^5D_3$ states increases as the Tb^{3+} increase up to 3.0 mol % owing to non-radiative from $^5D_3$ to $^5D_4$ states producing intense green emission for the

laser. Hence these glasses are potential candidate as a medium for green solid-state lasers.

Acknowledgement

The authors acknowledge the financial support from RMC, UTM through the research grant (VOTE: 4B329, 13J81 and 16H41).

References

[1] N. Effendy, Z.A. Wahab, S. Abdul Aziz, K.A. Matori, M.H.M. Zaid, S.S.A. Rashid, Characterization and optical properties of erbium oxide doped ZnO–SLS glass for potential optical and optoelectronic materials, Mater. Express. 7 (2017) 59–65. doi:10.1166/mex.2017.1328.

[2] N.A.M. Adnan, M.R. Sahar, M.S. Rohani, Optical Absorption in Erbium Doped Phosphate Glass Embedded with Cobalt Nanoparticles, Adv. Mater. Res. 1107 (2015) 409–414. doi:10.4028/www.scientific.net/AMR.1107.409.

[3] M.V.N.P. Rao, V. Ravikumar, L.S. Rao, P.V. Rao, M.S. Reddy, N. Veeraiah, Copper ion as a structural probe in PbO – CaF_2 – P_2O_5 glass system by means of spectroscopic and dielectric studies, 472 (2009) 489–496. doi:10.1016/j.jallcom.2008.05.011.

[4] M.R. Dousti, S.K. Ghoshal, R.J. Amjad, M.R. Sahar, F. Nawaz, R. Arifin, Structural and optical study of samarium doped lead zinc phosphate glasses, Opt. Commun. 300 (2013) 204–209. doi:10.1016/j.optcom.2013.02.043.

[5] J. Sułowska, I. Wacławska, M. Szumera, Comparative study of zinc addition effect on thermal properties of silicate and phosphate glasses, J. Therm. Anal. Calorim. 123 (2016) 1091–1098. doi:10.1007/s10973-015-5044-8.

[6] S.S. Sastry, B.R. Venkateswara, Spectroscopic studies of copper doped alkaline earth lead zinc phosphate glasses, Phys. B Phys. Condens. Matter. 434 (2014) 159–164. doi:10.1016/j.physb.2013.11.017.

[7] S.F. Khor, Z.A. Talib, W.M. Mat Yunus, Optical properties of ternary zinc magnesium phosphate glasses, Ceram. Int. 38 (2012) 935–940. doi:10.1016/j.ceramint.2011.08.013.

[8] K. El-Egili, H. Doweidar, Y.M. Moustafa, I. Abbas, Structure and some physical properties of PbO-P_2O_5 glasses, Phys. B Condens. Matter. 339 (2003) 237–245. doi:10.1016/j.physb.2003.07.005.

[9] S.A.M. Azmi, M.R. Sahar, Optical response and magnetic characteristic of samarium doped zinc phosphate glasses containing nickel nanoparticles, J. Magn. Magn. Mater. 393 (2015) 341–346. doi:10.1016/j.jmmm.2015.06.001.

[10] H. Takebe, Dissolution behavior of ZnO – P_2O_5 glasses in water, 352 (2006) 3088–3094. doi:10.1016/j.jnoncrysol.2006.04.002.

[11] J.G. Bunzli, S. Comby, A. Chauvin, C.D.B. Vandevyver, New Opportunities for Lanthanide Luminescence, J. Rare Earths. 25 (2007) 257–274. doi:10.1016/S1002-0721(07)60420-7.

[12] M.R. Dousti, R.J. Amjad, Enhanced green emission of terbium-ions-doped phosphate glass embedding metallic nanoparticles, J. Nanophotonics. 9 (2015) 93068. doi:10.1117/1.JNP.9.093068.

[13] P. Yasaka, J. Kaewkhao, Luminescence from lanthanides-doped glasses and applications: A review, Proc. - 2015 4th Int. Conf. Instrumentation, Commun. Inf.

Technol. Biomed. Eng. ICICI-BME 2015. (2016) 4–15. doi:10.1109/ICICI-BME.2015.7401304.

[14] C.G. Atkins, J.F. Massicott, J.R. Armitage, R. Wyatt, B.J. Ajnslie, S.P. Craig-Ryan, High-gain, broad spectral bandwidth erbium-doped fibre amplifier pumped near 1.5μm, Electron. Lett. 25 (1989) 910. doi:10.1049/el:19890610.

[15] L. Zhang, M. Peng, G. Dong, J. Qiu, An investigation of the optical properties of Tb^{3+} -doped phosphate glasses for green fiber laser, Opt. Mater. (Amst). 34 (2012) 1202–1207. doi:10.1016/j.optmat.2012.01.031.

[16] A N. Meza-rocha, G.H. Muñoz, a Speghini, M. Bettinelli, U. Caldiño, Neutral and warm white light emission in Tb^{3+}/Sm^{3+} zinc phosphate glasses, Opt. Mater. (Amst). 47 (2015) 537–542. doi:10.1016/j.optmat.2015.06.035.

[17] C.R. Kesavulu, A.C. Almeida Silva, M.R. Dousti, N.O. Dantas, A. S.S. de Camargo, T. Catunda, Concentration effect on the spectroscopic behavior of Tb^{3+} ions in zinc phosphate glasses, J. Lumin. 165 (2015) 77–84. doi:10.1016/j.jlumin.2015.04.012.

[18] D. He, C. Yu, J. Cheng, S. Li, L. Hu, Effect of Tb^{3+} concentration and sensitization of Ce^{3+} on luminescence properties of terbium doped phosphate scintillating glass, J. Alloys Compd. 509 (2011) 1906–1909. doi:10.1016/j.jallcom.2010.10.085.

[19] S.F. Ismail, M.R. Sahar, S.K. Ghoshal, Materials Characterization Physical and absorption properties of titanium nanoparticles incorporated into zinc magnesium phosphate glass, Mater. Charact. 111 (2016) 177–182. doi:10.1016/j.matchar.2015.11.030.

[20] Z.A.S. Mahraz, M.R. Sahar, S.K. Ghoshal, Reduction of non-radiative decay rates in boro-tellurite glass via silver nanoparticles assisted surface plasmon impingement: Judd Ofelt analysis, J. Lumin. 190 (2017) 335–343. doi:10.1016/j.jlumin.2017.05.059.

[21] A.H. Hammad, A.M. Abdelghany, Optical and structural investigations of zinc phosphate glasses containing vanadium ions, J. Non. Cryst. Solids. 433 (2016) 14–19. doi:10.1016/j.jnoncrysol.2015.11.016.

[22] M.R. Dousti, R.J. Amjad, Spectroscopic properties of Tb^{3+} -doped lead zinc phosphate glass for green solid state laser, J. Non. Cryst. Solids. 420 (2015) 21–25. doi:10.1016/j.jnoncrysol.2015.04.002.

[23] R. Arifin, N.A. Zulkifeli, M.R. Sahar, S.K. Ghoshal, ZnO Nanoparticles Concentration Dependent Optical Properties of Erbium Doped Phosphate Glass, Adv. Mater. Res. 1107 (2015) 471–476. doi:10.4028/www.scientific.net/AMR.1107.471.

[24] M. Elisa, B. a Sava, I.C. Vasiliu, R.C.C. Monteiro, C.R. Iordanescu, I.D. Feraru, L. Ghervase, C. Tanaselia, M. Senila, B. Abraham, Investigations on optical, structural and thermal properties of phosphate glasses containing terbium ions, IOP Conf. Ser. Mater. Sci. Eng. 47 (2013) 12025. doi:10.1088/1757-899X/47/1/012025.

[25] M. Reza Dousti, R.J. Amjad, Spectroscopic properties of Tb^{3+}-doped lead zinc phosphate glass for green solid state laser, J. Non. Cryst. Solids. 420 (2015) 21–25. doi:10.1016/j.jnoncrysol.2015.04.002.

[26] S.W. Yung, H.Y. Chiang, Y.S. Lai, F.B. Wu, C. Fu, Y. Lee, Thermal , optical and structural properties of Tb doped zinc aluminum phosphate glasses, 41 (2015) 877–888.

[27] M. Anand Pandarinath, G. Upender, K. Narasimha Rao, D. Suresh Babu, Thermal, optical and spectroscopic studies of boro-tellurite glass system containing ZnO, J. Non. Cryst. Solids. 433 (2016) 60–67. doi:10.1016/j.jnoncrysol.2015.11.028.

[28] G. Gao, A. Winterstein-Beckmann, O. Surzhenko, C. Dubs, J. Dellith, M.A. Schmidt, L. Wondraczek, Faraday rotation and photoluminescence in heavily Tb^{3+}-doped GeO_2-B_2O_3-Al_2O_3-Ga_2O_3 glasses for fiber-integrated magneto-optics, Sci. Rep. 5 (2015) 1–6. doi:10.1038/srep08942.

[29] Q. Chen, Q. Chen, H. Wang, G. Wang, S. Yin, Magneto optical properties of rare earth Tb_2O_3 doped PbO-Bi_2O_3 -B_2O_3 glass, J. Non. Cryst. Solids. 470 (2017) 99–107. doi:10.1016/j.jnoncrysol.2017.05.008.

[30] W. Ahmina, M. El Moudane, M. Zriouil, M. Taibi, Glass-forming region, structure and some properties of potassium manganese phosphate glasses, Phase Transitions. 1594 (2016) 1–11. doi:10.1080/01411594.2016.1144057.

[31] K. Mariselvam, R.A. Kumar, Borate Glasses for Luminescence Applications – Potential Materials for White LEDs and Laser Sources, Univers. J. Chem. 4 (2016) 55–64. doi:10.13189/ujc.2016.040202.

[32] J. Yang, L. Luo, Z. Chen, X. Chen, X. Tang, Tb-doped YPO_4 phosphors : Polyacrylamide gel synthesis and optical properties, J. Alloys Compd. 689 (2016) 837–842. doi:10.1016/j.jallcom.2016.08.065.

[33] G.R. Dillip, C.M. Reddy, M. Rajesh, S. Chaurasia, B.D.P. Raju, S.W. Joo, Green fluorescence of terbium ions in lithium fluoroborate glasses for, Bull. Mater. Sci. 39 (2016) 711–717. doi:10.1007/s12034-016-1192-0.

[34] B.C. Jamalaiah, J.S. Kumar, A.M. Babu, T. Sasikala, L.R.M. Ã, Study on spectroscopic and fluorescence properties of Tb^{3+} -doped LBTAF glasses, Phys. B Condens. Matter. 404 (2009) 2020–2024. doi:10.1016/j.physb.2009.03.037.

[35] M.M.E. A. Abdel-Kader, A. A. Higazy, Optical absorption studies for TeO_2-P_2O_5 and Bi_2Os-TeO_2-P_2O_5 glasses, J. Mater. Sci. 2 (1991) 204–208.

[36] H. Guo, Y. Wang, Y. Gong, H. Yin, Z. Mo, Y. Tang, L. Chi, Optical band gap and photoluminescence in heavily Tb^{3+} doped GeO_2 -B_2O_3 -SiO_2 -Ga_2O_3 magneto-optical glasses, J. Alloy. Compd. J. 686 (2016) 635–640. doi:10.1016/j.jallcom.2016.06.074.

[37] A.J. Silversmith, D.M. Boye, K.S. Brewer, C.E. Gillespie, Y. Lu, D.L. Campbell, $^5D_3 \rightarrow {}^7F_J$ emission in terbium-doped sol-gel glasses, J. Lumin. 121 (2006) 14–20. doi:10.1016/j.jlumin.2005.09.009.

[38] S.H. Bindu, D.S. Raju, V.V. Krishna, C.L. Raju, Preparation and characterization of Tb^{3+} ions doped zincborophosphate glasses for green emission, AIP Conf. Proceeding. 20003 (2017) 20002. doi:10.1063/1.4984149.

[39] M.A. Marzouk, S.M. Abo-naf, H.A. Zayed, N.S. Hassan, Photoluminescence and semiconducting behavior of Fe, Co, Ni and Cu implanted in heavy metal oxide glasses, J. Mater. Res. Technol. 5 (2015) 226–233.

[40] S.M. Hsu, S.W. Yung, Y.C. Hsu, F.B. Wu, C. Fu, Y.S. Lai, Y.M. Lee, Enhancement of luminescence properties and the role of ZnO in Tb^{3+} ions doped zinc aluminum phosphate glasses, Ceram. Int. 42 (2016) 4019–4025. doi:10.1016/j.ceramint.2015.11.071.

[41] W. A. Pisarski, L. Żur, T. Goryczka, M. Sołtys, J. Pisarska, Structure and spectroscopy of rare earth – Doped lead phosphate glasses, J. Alloys Compd. 587 (2014) 90–98. doi:10.1016/j.jallcom.2013.10.106.

[42] N.S. Hussain, Y.P. Reddy, S. Buddhudu, Emission properties of Tb^{3+} -doped zinc boro-silicate glasses, Mater. Lett. (2001) 303–308.

[43] C.H. Kam, S. Buddhudu, Luminescence and decay behaviour of Tb^{3+}:ZrF_4-BaF_2-LaF_3-YF_3-AlF_3-NaF optical glasses, Phys. B Condens. Matter. 337 (2003) 237–244. doi:10.1016/S0921-4526(03)00409-5.

[44] D. Umamaheswari, B.C. Jamalaiah, T. Sasikala, T. Chengaiah, I.G. Kim, L. Rama Moorthy, Photoluminescence and decay behavior of Tb^{3+} ions in sodium fluoro-borate glasses for display devices, J. Lumin. 132 (2012) 1166–1170. doi:10.1016/j.jlumin.2011.12.080.

Highlight

- The new compositions of Tb^{3+} doped P_2O_5 –ZnO glasses are prepared using melt-quenching technique.
- The influence of Tb_2O_3 concentration on physical, structural, thermal and photoluminescence behaviour are evaluated
- These glasses possess good chemical durability and rare earth solubility.
- Sample with 1.5 % possess highest thermal stability
- Enhanced intense green and mild blue emissions are observed with increment of Tb_2O_3 concentration in the glass system.
- Sample with 3.0 mol% Tb_2O_3 emit the most intense green colour and sample with 1.0 mol% Tb_2O_3 emit the most intense blue colour.
- These glasses display good optical characteristic and promising materials for green solid-state lasers.

Comprehensive study on compositional modification of Tb3+ doped zinc phosphate glass

ORIGINALITY REPORT

24%	17%	19%	6%
SIMILARITY INDEX	INTERNET SOURCES	PUBLICATIONS	STUDENT PAPERS

PRIMARY SOURCES

1	www.science.gov Internet Source	5%
2	Syariffah Nurathirah S. Yaacob, M.R. Sahar, E.S. Sazali, S. Sulhadi. "The Polarizability and Optical Characteristics of Zinc Phosphate Glasses Doped Terbium Embedded with Copper Oxide Nanoparticles", Solid State Phenomena, 2019 Publication	3%
3	1library.net Internet Source	2%
4	daneshyari.com Internet Source	2%
5	Zahra Ashur Said Mahraz, M.R. Sahar, S.K. Ghoshal. "Reduction of non-radiative decay rates in boro-tellurite glass via silver nanoparticles assisted surface plasmon impingement: Judd Ofelt analysis", Journal of Luminescence, 2017 Publication	2%

6	Puzi Anigrahawati, M.R. Sahar, S.K. Ghoshal. "Influence of Fe3O4 nanoparticles on structural, optical and magnetic properties of erbium doped zinc phosphate glass", Materials Chemistry and Physics, 2015 Publication	2%
7	Submitted to Brown University Student Paper	1%
8	N.M. Yusoff, M.R. Sahar. "Effect of silver nanoparticles incorporated with samarium-doped magnesium tellurite glasses", Physica B: Condensed Matter, 2015 Publication	1%
9	Himani Tiwari, Charu Chandra Dhondiyal. "Physical and optical analysis of Sm3+ doped zinc phosphate glass", Materials Today: Proceedings, 2021 Publication	1%
10	www.scientific.net Internet Source	1%
11	coek.info Internet Source	1%
12	Anastasiia Babkina, Ekaterina Kulpina, Yevgeniy Sgibnev, Yuriy Fedorov et al. "Terbium concentration effect on magneto-optical properties of ternary phosphate glass", Optical Materials, 2020	1%

Publication

13	Dousti, M. Reza, S.K. Ghoshal, Raja J. Amjad, M.R. Sahar, Fakhra Nawaz, and R. Arifin. "Structural and optical study of samarium doped lead zinc phosphate glasses", Optics Communications, 2013. Publication	<1 %
14	M. Reza Dousti, S.K. Ghoshal, Raja J. Amjad, M.R. Sahar, Fakhra Nawaz, R. Arifin. "Structural and optical study of samarium doped lead zinc phosphate glasses", Optics Communications, 2013 Publication	<1 %
15	Marta Sołtys, Joanna Pisarska, Magdalena Leśniak, Maciej Sitarz, Wojciech A. Pisarski. "Structural and spectroscopic properties of lead phosphate glasses doubly doped with Tb 3+ and Eu 3+ ions", Journal of Molecular Structure, 2018 Publication	<1 %
16	Syariffah Nurathirah Syed Yaacob, Md. Rahim Sahar, Faizani Mohd Noor, Nur Liyana Amiar Rodin et al. "Comparative Spectroscopic Studies on Luminescence Performance of Er^{3+} Doped Tellurite Glass Embedded with Different Nanoparticles (Ag Co and Fe) at 0.55 μm Emission", Solid State Phenomena, 2021 Publication	<1 %

17	assets.researchsquare.com Internet Source	<1 %
18	www.sparrho.com Internet Source	<1 %
19	Submitted to University of Hong Kong Student Paper	<1 %
20	journal.masshp.net Internet Source	<1 %
21	Inaba, S.. "Heat capacity of oxide glasses at high temperature region", Journal of Non-Crystalline Solids, 20030915 Publication	<1 %
22	res.mdpi.com Internet Source	<1 %
23	mafiadoc.com Internet Source	<1 %
24	www.hindawi.com Internet Source	<1 %
25	Submitted to Universiti Teknologi MARA Student Paper	<1 %

Exclude quotes	On	Exclude matches	< 15 words
Exclude bibliography	On		